UDC 551.558.1

INTERACTIONS BETWEEN THE VELOCITY FIELDS OF SUCCESSIVE THERMALS

EUGENE M. WILKINS,[1] YOSHIKAZU SASAKI, and ROGER H. SCHAUSS
University of Oklahoma, Norman, Okla.

ABSTRACT

Solitary thermals and continuous plume thermals both occur in nature, and the intermediate case of interacting successive thermals in a series may also be an important part of atmospheric convection. This analysis shows that residual updraft and vorticity concentration in the wake of a preceding thermal can have important effects on its successor.

A fluid mechanics model of buoyant clouds rising through a rotating medium is constructed for the purpose of predicting some of the sequential thermal effects that can be measured quantitatively for thermals simulated in the laboratory. The agreement with theory is satisfactory for the parameters that are subject to measurement, but some relevant constants can only be determined experimentally.

For a situation in which a first thermal reacts strongly with the rotation field, it is shown that a succeeding thermal may receive a sizable enhancement of its vertical momentum even though its predecessor was suppressed by the interaction. These findings may be relevant to the generation and maintenance of small-scale atmospheric vortexes such as tornadoes, waterspouts, and dust devils.

1. INTRODUCTION

Numerical and laboratory simulations of successive thermals have been conducted to study the effects of wakes and the interactions of toroidal circulations whenever one buoyant element comes into the domain of another.

Some of the most important interaction effects may be distinguished according to the time interval between the departures of thermals from a heated surface. The extreme situation for long time intervals is the isolated and discrete buoyant element, and the situation approaches that of a continuous plume or jet as the time interval approaches zero. Between these extremes are three distinct classifications according to whether the time intervals are short, intermediate, or relatively long.

For "short" time intervals, a second thermal will have its rate of rise so enhanced by the updraft of its predecessor that the second will actually overtake the first. Depending on their relative torus diameters at this time, they will either coalesce into a single invigorated thermal or else the second one will pass through the center of the first one and continue upward in isolation.

"Intermediate" time intervals are typified by some enhancement of rise rate due to wake effect, but these do not result in overtaking or coalescing.

"Long" time intervals are classified as those for which the updraft in the wake has decayed to the point of ineffectiveness, but residual turbulence causes a more rapid dilution of a succeeding thermal than would be the case in the absence of a wake.

In the laboratory simulation experiments, but not necessarily in the real atmosphere, the latter two phases merge quite noticeably; and the effects of residual updraft and turbulence both govern the evolution of a second thermal.

When a rotating medium is considered, the series effect is more conveniently classified accordingly as the environmental field of vorticity is predominantly uniform ("solid" rotation) or irrotational (V–R vortex). Of course, the time interval between thermals gives an additional complexity; but its importance decreases somewhat in proportion to the magnitude of the rotation speed.

A theoretical analysis has yielded numerical predictions of successive thermal interaction effects, in both stationary and rotating media. This approach derives governing equations based on the conservation of volume, vertical momentum, angular momentum, and buoyancy, similar to the turbulent convection equations of Morton et al. (1956). Solutions are obtained for some cases and compared with simulations in the thermal tank.

Much can be learned from such experiments about the nature of successive thermal interactions and the resulting enhancements of velocity fields despite the inherent complexities and consequent oversimplifications.

The major simplifications are in the assumptions of:

1. Total buoyancy is invariant with time (adiabatic thermals).
2. First and succeeding thermals have the same initial buoyancy.
3. First and succeeding thermals originate from the same spot and follow the same path.
4. Turbulent exchange at the periphery of the thermal is not taken into account explicitly.
5. The thermals are axially symmetrical.

This paper is an extension of the research reported by Wilkins et al. (1969) dealing with rotation-influenced solitary thermals. The previous work showed that some of the important interactions occurring in laboratory simulations of the phenomenon could be predicted by a theory derived from equations stating the conservation of cloud volume, buoyancy, vertical momentum, and

[1] Also at the LTV (Ling-Temco-Vought, Inc.) Research Center, Dallas, Tex.

angular momentum. The volume and vertical growth were measured quantitatively for the simulated clouds, and these measurements compared very well with theory. For some combinations of cloud buoyancy and ambient vorticity, a concentrated votex was seen to form in the wake of the thermal. Vortex-forming interactions of this kind were found to suppress the vertical growth of the cloud by a predictable amount, although one of the parameters of the theory, the radius of entrainment, had to be estimated from the experimental results.

In extending the theory to attack the problem of successive thermals, we consider the effect on a thermal of encountering the wake from a preceding thermal. In the first situation, we assume that the vorticity field is essentially the same for both thermals, and in the second situation we assume that the first thermal reacts strongly with the rotation field; this rearrangement of the ambient vorticity gives an important change of environment for the second thermal, and the analysis will attempt to predict some of the consequences.

2. THEORY

The equations of Morton et al. (1956) expressing the conservation of volume, vertical momentum, and buoyancy in a thermal cloud were modified by Wilkins et al. (1969) to take into account the effect on momentum of an interaction of the thermal's toroidal circulation with a rotating environment. These equations apply to an "adiabatic" thermal or a thermal in which the total buoyancy does not change with time. This is comparable to a dry thermal in a neutrally stable atmosphere or to our laboratory experimental thermal, created by injecting a detergent foam into a tank of water. The modified equations are:

$$\text{volume} \qquad \frac{d}{dt}\left(\frac{4}{3}\pi b^3\right)=4\pi b^2 \alpha w, \tag{1}$$

$$\text{momentum} \qquad \frac{d}{dt}\left(\frac{4}{3}\pi b^3 w\right)=\frac{4}{3}\pi b^3\Delta+\underline{\frac{4}{3}\pi b^3\omega}, \tag{2}$$

and

$$\text{buoyancy} \qquad \frac{d}{dt}\left(\frac{4}{3}\pi b^3\Delta\right)=0; \tag{3}$$

the new term has been underlined. The assumptions about preservation of shape, velocity distribution, and entrainment proportional to vertical velocity w through an entrainment constant α are the same as in Morton et al. (1956). For simplicity, a sphere-equivalent radius b is used throughout, even though the cloud shape is not in general spherical. Turner (1964) has shown that the shape factor is negligible in the case of the spheroidal clouds simulated in the laboratory. The entrainment constant α relates inflow velocity to thermal cap velocity. The density-deficit buoyancy acceleration is

$$\Delta=g(\rho_0-\rho)/\rho_0 \tag{4}$$

where g is gravitational acceleration, ρ is cloud density, and ρ_0 is the density of the environmental fluid. An acceleration ω arises from the changes that occur in the vertical gradient of pressure as a result of rearrangement of the velocity field when vortex formation occurs; tangential velocity increases owing to conservation of angular momentum in fluid entrained by the thermal. The derivation by Wilkins et al. (1969) shows that the form taken by the solutions to the conservation eq (1–3) depends on the assumption made about R, the entrainment radius or "reach" of the thermal into its environment. This radius has the same meaning here as in Kuo (1966). Solutions were obtained for two cases: (A) one in which R (=constant) is assumed not to vary with height and (B) one in which R is assumed to be proportional to the sphere-equivalent radius b through a constant γ. These two cases will also be used to analyze successive thermals in a rotating medium. In each case, the solutions for a solitary thermal will be given first for comparison purposes and also because these solutions will be needed for the purpose of analyzing successive thermals.

SOLUTIONS FOR (A)

For a solitary thermal, the rotation-induced vertical acceleration ω was found by Wilkins et al. (1969) to be

$$\omega=\Lambda_1^2\cdot\frac{1}{b^3}\frac{db}{dz} \tag{5}$$

where z is the vertical coordinate and

$$\Lambda_1^2=3.6R^4\Omega^2 \tag{6}$$

where Ω is the constant angular velocity of the rotating environment. The factor 3.6 is $-1+2\cdot\log 10$ where 10 represents the ratio of sphere-equivalent radius to a small critical radius; this ratio is not important to the present analysis.

The solutions to the conservation equations for the solitary thermal are

$$b=At^{1/2},$$

$$w=\frac{1}{2\alpha}At^{-1/2},$$

$$\Delta=(3F/4\pi A^3)t^{-3/2},$$

$$E=\frac{3}{2}t^{-1}=\text{entrainment rate},$$

$$A=[(3\alpha F/2\pi)-2\Lambda_1^2\alpha^2]^{1/4},$$

$$F=\frac{4}{3}\pi b^3\Delta=\text{constant buoyancy force},$$

and

$$h=\frac{b}{\alpha}=\text{height of thermal cap.} \tag{7}$$

Solutions for a nonrotating fluid are obtained by setting $\Lambda_1=0$. Since Λ_1^2 is nonnegative, suppression of the thermal's growth occurs as a result of rotation, regardless of the direction. Note that the entrainment rate is independent of rotation for the simpler case of $R=\text{const}$; some justification for this case is seen in the fact that the entrainment rate was also not affected by rotation for the simulated thermals reported by Wilkins et al. (1969).

Successive thermals. In addition to the assumptions mentioned earlier, the following new assumptions are introduced for the purpose of analyzing the interactions between thermals in a series:

1. The wake velocity of a preceding thermal possesses the same "top hat" velocity profile as its thermal cap.
2. The wake velocity decays according to the same law as obtained for the thermal cap.

The latter assumption is a key one for the theoretical development to follow. Other schemes have been tried for the wake velocity configuration, but the one above is most consistent for use with a modification of the existing theory.

According to this reasoning, the wake updraft W, residual from a preceding thermal of cap velocity w_1, will have a magnitude proportional to w_1 corrected for a prior decay time τ, which is just the delay time between thermals. The vertical velocity w_1 for the first thermal is placed in the proper time frame for the second one if time t in equation set (7) is replaced by $t+\tau$, so that

$$w_1=\frac{1}{2\alpha}A(t+\tau)^{-1/2}. \tag{8}$$

Since the radial growth of a succeeding thermal is not at all constrained to be the same as its predecessor, it is logical to expect that the wake effect must somehow depend on the ratio b/b_1, where again the subscript 1 applies to a preceding thermal. We observe qualitatively in simulation experiments that the magnitude of the thermal's response to the wake apparently is proportional not only to w_1 but also to the amount of the wake occupied by the thermal, suggesting that wake velocity varies with radius. This is an important consideration for thermals in a rotating medium because the thermal's radius is strongly affected by the interaction with the rotation field. Assuming the wake effect to be proportional to b/b_1 also makes the problem tractable, although elsewhere the theoretical model assumes the vertical velocity to be constant across the thermal. This ratio may be regarded somewhat as a correction factor. The top-hat velocity profile assumption is a useful one; apparently its lack of realism introduces little error in the analysis of solitary thermals, as evidenced in the experiments reported by Scorer (1957), Turner (1963), and Wilkins et al. (1969). The wake radius will be given by

$$b_1=A(t+\tau)^{1/2} \tag{9}$$

to be consistent with the assumption about w_1, and thus

$$W\propto\frac{b}{b_1}w_1=\frac{\beta b}{2\alpha}(t+\tau)^{-1} \tag{10}$$

where β is a constant of proportionality in which the magnitude can only be inferred from experimental data.

The modifications to the conservation eq (1–3) are now quite straightforward. The first equation in the set is not affected, since entrainment is assumed to be proportional only to the vertical velocity w of the thermal relative to the wake in which the thermal is imbedded. In the second equation, the total momentum (per unit mass) due to both vertical velocities (w and W) must be conserved by balancing the forces due to buoyancy and rotation suppression. The third equation is unaffected. The new equations are

$$\frac{d}{dt}\left(\frac{4}{3}\pi b^3\right)=4\pi b^2\alpha w, \tag{11}$$

$$\frac{d}{dt}\left[\frac{4}{3}\pi b^3(w+W)\right]=\frac{4}{3}\pi b^3\Delta-\frac{4}{3}\pi b^3\Lambda_2^2\cdot\frac{1}{b^3}\frac{db}{dz}, \tag{12}$$

and

$$\frac{d}{dt}\left(\frac{4}{3}\pi b^3\Delta\right)=0,\qquad F=\frac{4}{3}\pi b^3\Delta=\text{const.} \tag{13}$$

From eq (11) and the relation

$$\frac{db}{dt}=(w+W)\frac{db}{dz}, \tag{14}$$

we obtain

$$\frac{db}{dz}=\frac{\alpha w}{w+W}. \tag{15}$$

Because of velocity decay in the wake, we can assume that W is considerably less than w, thus eq (12) is simplified by the substitution $\alpha=db/dz$. The conservation equations can now be combined to yield the linear second-order differential equation

$$\frac{d^2b^4}{dt^2}+2\beta(t+\tau)^{-1}\frac{db^4}{dt}-2\beta(t+\tau)^{-2}b^4=\frac{3\alpha F}{\pi}-4\alpha^2\Lambda_2^2. \tag{16}$$

This equation is placed in a more manageable form by nondimensionalizing the independent variable such that

$$\frac{t+\tau}{\tau}=x,\qquad \frac{d}{dx}=\tau\frac{d}{dt}. \tag{17}$$

When letting $y=b^4$, $\lambda=3\alpha F/\pi-4\alpha^2\Lambda_2^2$, and using primes to represent x derivatives, eq (16) can be written as

$$x^2y''+2\beta xy'-2\beta y=\lambda\tau^2x^2. \tag{18}$$

This equation has for a particular solution the function $\lambda\tau^2x^2/2(1+\beta)$, and the reduced equation is satisfied by a function of the form x^n, where

$$n=1,\quad -2\beta. \tag{19}$$

Thus the complete solution is written as

$$y=\frac{\lambda\tau^2x^2}{2(1+\beta)}+C_1x+C_2x^{-2\beta}. \tag{20}$$

The boundary conditions to be applied are consistent with those used by Wilkins et al. (1969) in the analysis of solitary thermals. The requirement that $y=0$ when $t=0$ (or $x=1$) gives

$$C_1=-(1+C_2) \tag{21}$$

so that

$$y=\frac{\lambda\tau^2}{2(1+\beta)}\,[x^2-(1+C_2)x+C_2x^{-2\beta}]. \tag{22}$$

The requirement that dy/dt (proportional to vertical momentum) be zero at $t=0$ gives

$$C_2=(1+2\beta)^{-1}, \tag{23}$$

so that finally

$$y=\frac{\lambda\tau^2}{2(1+\beta)}\left[x^2-\frac{2(1+\beta)x}{1+2\beta}+\frac{x^{-2\beta}}{1+2\beta}\right]. \tag{24}$$

Negative β is not excluded, but $\beta<0$ represents a downdraft in the wake. This situation is of only minor interest in this analysis, but we note that singularities exist for $\beta=-1$ and $\beta=-(1/2)$. These are special cases, requiring separate solutions to eq (18) which are not contained in (24). When applying the same boundary conditions as before, these solutions are

$$\beta=-1: \qquad y=\lambda\tau^2x^2\left(\ln x-1+\frac{1}{x}\right) \tag{25}$$

and

$$\beta=-\frac{1}{2}: \qquad y=\lambda\tau^2x^2\left(1-\frac{\ln x}{x}-\frac{1}{x}\right). \tag{26}$$

These solutions will show a suppression of the thermal even in the absence of rotation.

That eq (24) is a quite general solution to the problem of successive thermals in a rotating medium is seen in the fact that (24) contains as special cases all the solutions for the simpler situations. For example, the solutions for successive thermals in a nonrotating medium are obtained by setting $\Lambda_2=0$.

The solutions for a *solitary* thermal are obtained by setting $\beta=\tau=0$ in eq (24), which produces the set (7); this set contains as a special case the solution set for solitary thermals in a nonrotating medium.

Note that the rotation-effects constant Λ_2 applies to the second thermal, and the solution (24) for the case $R=$const is independent of any assumption as to whether or not $\Lambda_1=\Lambda_2$. This is not the case for R variable, as will be seen later. However, for the present case, the first thermal is supposed not to alter the ambient vorticity field appreciably, and so $\Lambda_1=\Lambda_2$ is not a bad assumption.

The expressions for w, h, E, *and* Δ may be calculated from the solution for y $(=b^4)$ in eq (24). For example,

$$w=\frac{1}{\alpha}\frac{db}{dt}=\frac{1}{2\alpha\tau}\left[\frac{\lambda\tau^2}{2(1+\beta)}\right]^{1/4}\left[x-\frac{(1+\beta)}{1+2\beta}-\frac{\beta x^{-(2\beta+1)}}{1+2\beta}\right]\times\left[x^2-\frac{2(\beta+1)x}{1+2\beta}+\frac{x^{-2\beta}}{1+2\beta}\right]^{-3/4}. \tag{27}$$

The height of rise h of the thermal cap as a function of time must be obtained from

$$h=\int_0^t (w+W)dt, \tag{28}$$

which can be written as

$$h=\frac{b}{\alpha}+\frac{\beta}{2\alpha}\int_1^x b\,\frac{dx}{x} \tag{29}$$

by substituting from eq (10), (11), and (17). The integral in eq (29) appears to represent that portion of the thermal's rise which has been added as a result of the presence of the wake; however, the radius b is also affected. The fourth-root polynomial in b makes the integration

$$\int_1^x\left[x^2-\frac{2(1+\beta)x}{1+2\beta}+\frac{x^{-2\beta}}{1+2\beta}\right]^{1/4}\cdot\frac{dx}{x}$$

very difficult to perform. For short times ($t\leq\tau$) and ($\beta<1$), it is possible to expand the polynomial and integrate term by term. This has been carried out by rejecting third and higher powers of β and t/τ, and eq (29) then becomes

$$h=\frac{b}{\alpha}+\frac{\beta}{2\alpha}\left[\frac{\lambda\tau^2}{2(1+\beta)}\right]^{1/4}\int_0^\xi\frac{\xi^{1/2}}{\xi+1}\left\{1+\frac{1}{2}\beta\left[\frac{1}{2}-\frac{1+\beta}{3}\xi+\left(\frac{1}{4}+\frac{5}{12}\beta\right)\xi^2-\cdots\right]\right\}d\xi \tag{30}$$

where the substitution $\xi=x-1$ has been made. The approximate expression for h is

$$h=\frac{b}{\alpha}+\frac{\beta}{2\alpha}\left[\frac{\lambda\tau^2}{2(1+\beta)}\right]^{1/4}\left[(\xi^{1/2}-\tan^{-1}\xi^{1/2})\cdot\left(2+\beta+\frac{3}{4}\beta^2\right)-\frac{1}{9}(\beta+\beta^2)^{3/2}+\frac{1}{4}\left(\beta+\frac{5}{3}\beta^2\right)\cdot\left(\frac{\xi^{5/2}}{5}-\frac{\xi^{3/2}}{3}\right)\right]. \tag{31}$$

SOLUTIONS FOR (B)

The assumption $R=\gamma b$ is reasonable, in that the radius of entrainment of the thermal is somehow related to the sphere-equivalent radius of the cloud, although the exact relationship is not known. In the case of a rotational environment, we know that lateral motions tend to be suppressed (Taylor-Proudman effect[2]), and we observe experimentally that the cloud appearance changes from spheroidal to narrow cylindrical as the rotational influence is increased. Unfortunately, this observation does not provide us with a prediction of the functional relationship between R and b, but it does indicate that R and the visible radius tend to vary in the same sense. Thus we consider the case $R=\gamma b$ (γ constant) while acknowledging that, in the case of strong rotational influence, it is possible that, owing to vertical stretching, the sphere-equivalent radius may increase while R remains constant or even decreases.

The rationale is the same as before for the modifications to the conservation equations. Again, we derive first the

[2] From (Taylor 1921, Proudman 1916, and Chandrasekhar 1961)

solutions for a solitary thermal, since these are used in the determination of the wake velocity present for the succeeding thermal. The vertical acceleration ω due to the rotation effect was derived by Wilkins et al. (1969) to be

$$\omega=-\Lambda_1^2 b\frac{db}{dz} \tag{32}$$

in eq (2), where

$$\Lambda_1^2=\gamma^2\Omega^2(5.6\gamma^2-1). \tag{33}$$

For the normal situation in which rotation suppresses the vertical motion of the cloud ($\Lambda_1^2<0$), the solutions for the solitary thermal were shown by Wilkins et al. (1969) to be

$$\begin{aligned}
&h=b/\alpha\\
&b=(3F/4\pi\alpha\Lambda_1^2)^{1/4}\,[1-\cos(2\alpha\Lambda_1 t)]^{1/4}\\
&w=\frac{1}{2}\,(3F\Lambda_1^2/4\pi\alpha)^{1/4}\sin(2\alpha\Lambda_1 t)\,[1-\cos(2\alpha\Lambda_1 t)]^{-3/4}\\
&\Delta=(3F\alpha^3\Lambda_1^6/4\pi)^{1/4}\,[1-\cos(2\alpha\Lambda_1 t)]^{-3/4}\\
\text{and}&\\
&E=\frac{3}{2}\alpha\Lambda_1\sin(2\alpha\Lambda_1 t)[1-\cos(2\alpha\Lambda_1 t)]^{-1}.
\end{aligned} \tag{34}$$

The solutions for rotational enhancement of vertical motion are similar to eq (34) except that the trigonometric functions are hyperbolic. Note that entrainment is affected by rotation for the case $R=\gamma b$, whereas it was not affected when $R=$const.

Successive thermals. The analysis proceeds exactly as before. The wake velocity W is given by

$$W=\beta w_1\frac{b}{b_1}=\frac{1}{2}\,\beta b\Lambda_1\cot\alpha\Lambda_1(t+\tau) \tag{35}$$

where w_1 and b_1 are obtained from the set (34) by replacing t with $t+\tau$. The momentum conservation equation comparable to eq (12) is

$$\frac{d}{dt}\left[\frac{4}{3}\,\pi b^3(w+W)\right]=\frac{4}{3}\,\pi b^3\Delta-\frac{4}{3}\,\pi b^4\Lambda_2^2\frac{db}{dz}. \tag{36}$$

This equation can be combined with the other conservation equations to obtain the linear second-order differential equation

$$\frac{d^2b^4}{dt^2}+2\beta\alpha\Lambda_1\cot\alpha\Lambda_1(t+\tau)\frac{db^4}{dt}-2\beta\alpha^2\Lambda_1^2\csc^2\alpha\Lambda_1(t+\tau)\cdot b^4+4\alpha^2\Lambda_2^2\cdot b^4=3\alpha F/\pi. \tag{37}$$

For $R=\gamma b$, the governing equation contains both Λ_1 and Λ_2, which certainly need not be equal. In the event (discussed later) that the preceding thermal reacts strongly with the rotation field, vorticity will become concentrated within the thermal's wake to such an extent that Λ_1 and Λ_2 may differ by more than a negligible amount, and the solution must be obtained from eq (37). If the interaction is not so strong that vortex formation occurs in the wake of the first thermal, then we can assume $\Lambda_1=\Lambda_2=\Lambda$, giving

$$\frac{d^2b^4}{dt^2}+2\beta\alpha\Lambda\cot\alpha\Lambda(t+\tau)\frac{db^4}{dt}+2\alpha^2\Lambda^2[2-\beta\csc^2\alpha\Lambda(t+\tau)]\cdot b^4=3\alpha F/\pi. \tag{38}$$

This equation is further simplified by the transformation

$$\zeta=\alpha\Lambda(t+\tau),\quad x=\cot\zeta \tag{39}$$

to obtain

$$(1+x^2)^2\frac{d^2b^4}{dx^2}+2x(1-\beta)(1+x^2)\frac{db^4}{dx}+2[2-\beta(1+x^2)]b^4=3F/\pi\alpha\Lambda^2. \tag{40}$$

A method of definite integrals may be applied to solve this equation, although it is probably more efficient to compute via finite-difference routine directly from eq (40).

3. ANALYSIS FOR THE CASE OF STRONG INTERACTION

We now consider the case where a preceding thermal has interacted with the rotating medium so as to form a concentrated vortex, thus rearranging the profile of tangential velocity from linear to hyperbolic (solid rotation to "irrotational" motion). The second buoyant element encounters an environment in which the vorticity is essentially zero over most of the region contacted by the thermal.

The derivation of the rotation effects term for the momentum conservation equation parallels that given by Wilkins et al. (1969). The environment is assumed to have a profile of tangential velocity with a maximum v_m at a small radius r_m. Prior to vortex formation, the velocity at that radius was Ωr_m, and afterward the expression

$$v_m r_m=\Omega R_1^2=V_\theta R_1 \tag{41}$$

states the principle of angular momentum conservation for the fluid entrained inward from an "effective radius" R_1 of the first thermal. The tangential velocity V_θ at radius R_1 is assumed to be unchanged by the process, since fluid moving into that location will come from above or below at the same radial distance R_1. Thus R_1 is a radius beyond which the influence of the thermal is negligible. This is consistent with the assumptions of Kuo (1966). At any radius r greater than r_m, the tangential velocity is given by

$$v_\theta r=v_m r_m. \tag{42}$$

The second thermal will entrain fluid from a distance R_2 which is not necessarily the same as R_1. Bernoulli's law can be used to predict the form of the total energy conserved in the environment of the second thermal. The pressure distribution must conform to the velocity distribution such that

$$\frac{1}{2}(v_\theta^2+v_r^2)+\frac{p_1}{\rho}=\frac{1}{2}(V_\theta^2+V_r^2)+\frac{p_2}{\rho_0} \tag{43}$$

where v_r and V_r are the radial components of the velocities at the radii r and R_2, respectively, and p_1 and p_2 are the fluid pressures inside and outside the thermal, respectively. In the case of strong interaction, there must be considerable convergence; and therefore, for simplicity, we will assume that the two velocity components are equal. Equation (43) can be written as

$$\frac{p_1}{\rho}=\frac{p_2}{\rho_0}+\Omega^2R_1^4\left(\frac{1}{R_2^2}-\frac{1}{r^2}\right). \tag{44}$$

The average value of p_1 (designated $\bar{p}_1$) inside the thermal cloud can be found by integrating p_1 over the area included between r_m and b; we assume that the region between $r=0$ and $r=r_m$ is negligibly small. Hence

$$\frac{\bar{p}_1}{\rho}=\frac{1}{\pi(b^2-r_m^2)}\int_{r_m}^{b}\frac{p_1}{\rho}\cdot 2\pi r dr$$

$$=\frac{p_2}{\rho_0}+\Omega^2R_1^4\left(\frac{1}{R_2^2}-\frac{2\log\frac{b}{r_m}}{b^2-r_m^2}\right). \tag{45}$$

The following assumptions have the purpose of making the problem tractable. While these assumptions are not proved, they are all consistent with the rationale stated earlier for the situation of strong interaction between the toroidal circulation of the thermal and the ambient vorticity field.

1. The cloud radius b is 10 times larger than r_m, so that $\log b/r_m=2.3$. Therefore, r_m^2 can be neglected in comparison to b^2.

2. Experimentally, we observe the cloud to be cylindrical for the case of strong interaction, and this indicates that R_1=const for the first thermal. There is not sufficient observational data to suggest a functional form for R_2 (second thermal), but we will relate R_2 to the sphere-equivalent cloud radius as before ($R_2=\gamma b$). With these assumptions, the last equation can be written as

$$\frac{\bar{p}_1}{\rho}=\frac{p_2}{\rho_0}+\Omega^2R_1^4\left(\frac{1}{\gamma^2}-2\log\frac{b}{r_m}\right)\frac{1}{b^2}. \tag{46}$$

The difference between the vertical gradient of pressure inside and outside the thermal is a measure of the rotation-induced vertical acceleration that we are seeking. Thus we have

$$\frac{d}{dz}\left(\frac{\bar{p}_1}{\rho}\right)=-g-2\Omega^2R_1^4\left(\frac{1}{\gamma^2}-3.6\right)\cdot\frac{1}{b^3}\frac{db}{dz}, \tag{47}$$

and the rotation-induced vertical acceleration can then be written as

$$\omega=\Lambda_2^2\cdot\frac{1}{b^3}\cdot\frac{db}{dz} \tag{48}$$

where

$$\Lambda_2^2=2\Omega^2R_1^4\left(\frac{1}{\gamma^2}-3.6\right) \tag{49}$$

and Λ_2^2 can be either positive or negative, depending on the magnitude of γ. Experiments with *solitary* thermals in a rotating medium (Wilkins et al. 1969) showed that γ was less than 0.5. The critical value of γ in eq (49) is 0.526; larger values will give suppression of the cloud's vertical motion, and smaller values give *enhancement.* This is to be contrasted with the situation for "solid rotation" (eq 33) in which the critical value of γ is 0.42; *smaller* values of γ result in *suppression* of the vertical momentum in this case. This is an important distinction between the two different kinds of ambient vorticity fields.

The equation for the conservation of vertical momentum now reverts to the simpler form of eq (12) rather than (36). The definition of the wake velocity W is given by eq (10) for the case R_1=const, and combining the three conservation equations gives the linear second-order differential equation

$$\frac{d^2b^4}{db^2}+2\beta(t+\tau)^{-1}\frac{db^4}{dt}-2\beta(t+\tau)^{-2}b^4=\frac{3\alpha F}{\pi}\pm4\alpha^2\Lambda_2^2. \tag{50}$$

Formally, this equation is solved in the same manner as eq (16). Of course, the definition of the rotation effects term Λ_2 is now entirely different and contains one additional empirical parameter γ. Refer to eq (24–31) for the solutions to eq (50).

4. LABORATORY SIMULATIONS

The laboratory apparatus is the thermal tank and turntable shown in figure 1. The tank (a) is 183 cm deep and 75 cm in diameter and is fabricated of 1.25-cm Plexiglas.[3] The tank is filled with water to 90-percent capacity, and injections of buoyant material are made through an orifice in the bottom of the tank through a 300-cm³ stainless steel syringe (b). The syringe is controlled remotely at console (c) by means of a solenoid valve, which releases compressed air to drive the piston of the syringe. The Nikon FT 35-mm camera with electric drive (d) used to record data is also controlled at this console, as is the motor drive for the turntable. An exposure rate of two frames per second was used for recording the evolution of the cloud, and a photogrammetric method (Wilkins et al. 1969) was used to eliminate distortion and obtain the volume of the cloud as a function of time. For rotation experiments, the camera rotates with the tank and thus sees only the relative vorticity created by the interaction of the thermal with the rotation

[3] Mention of a commercial product does not constitute an endorsement.

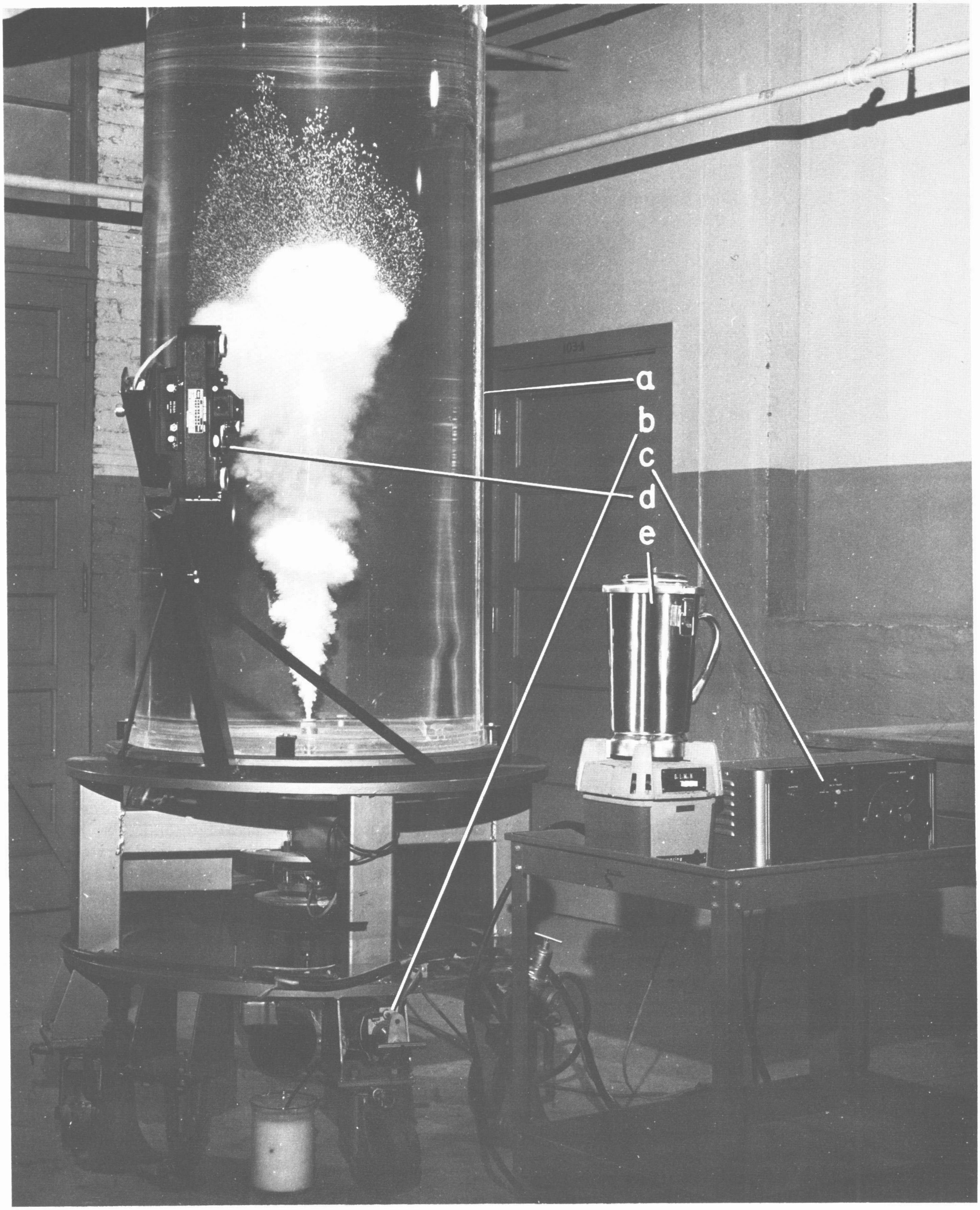

FIGURE 1.—Experimental apparatus.

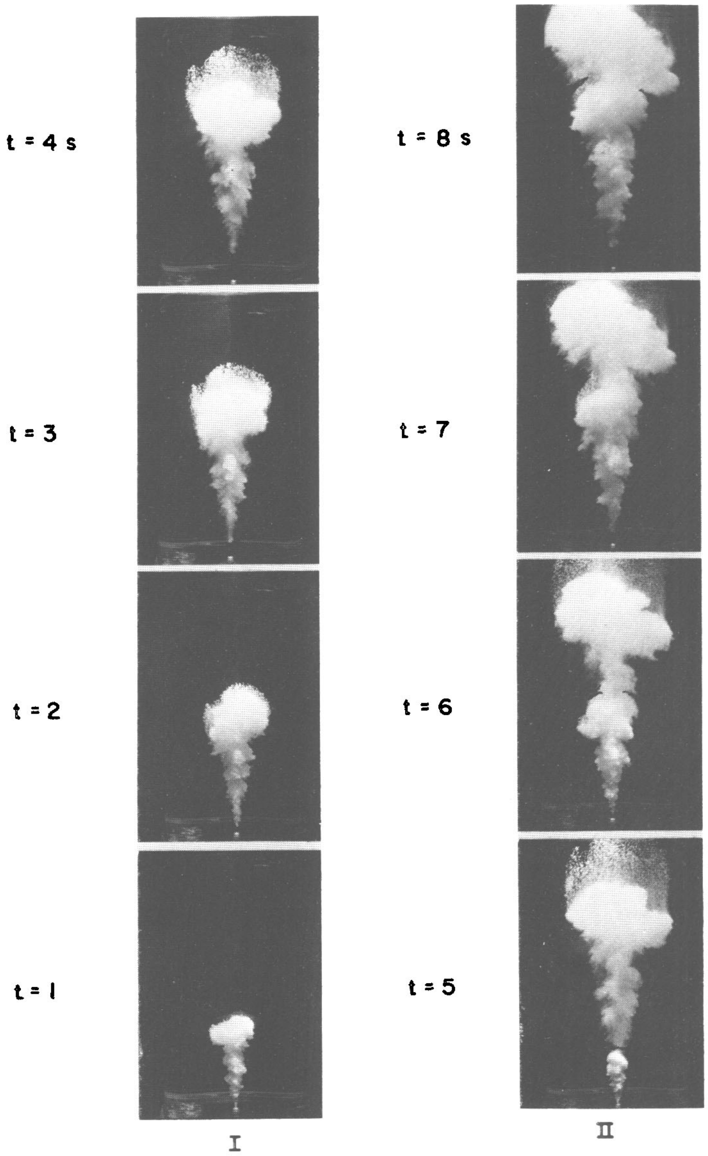

FIGURE 2.—Photographic sequence showing a second thermal (column II) released into the wake of a preceding thermal 4.5 s after the initial injection.

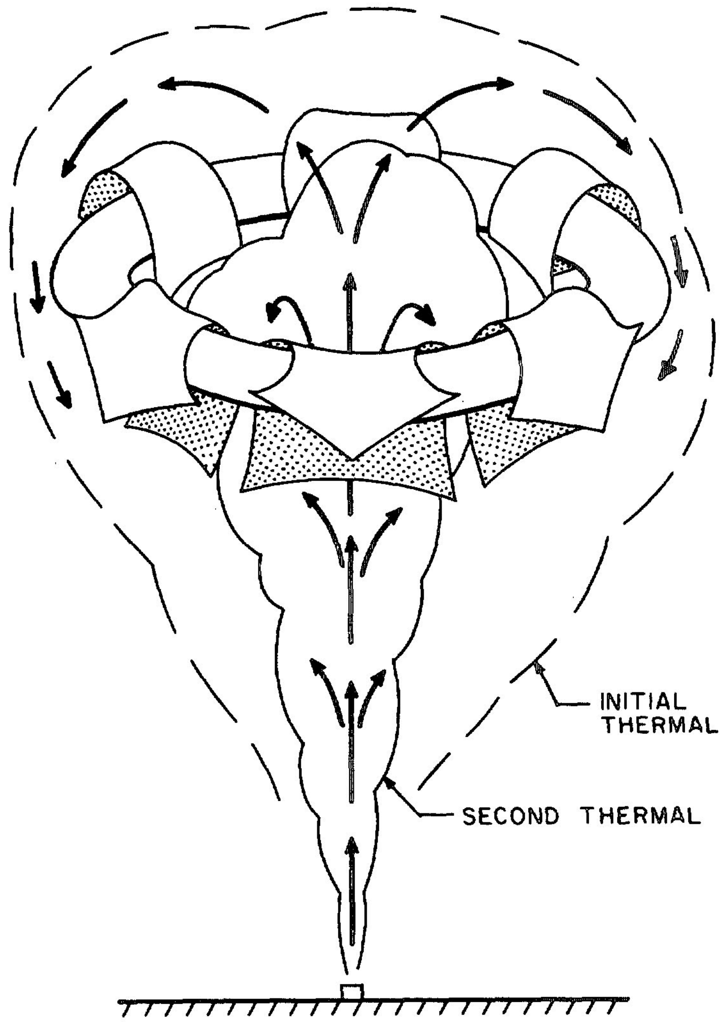

FIGURE 3.—Schematic diagram showing the toroidal circulations of a first thermal and an overtaking second thermal.

field. The sphere-equivalent radius b and the entrainment rate E were calculated directly from these measurements. The only other quantity measured quantitatively was the height h of the thermal cap. More details of the experimental methods are given in Wilkins et al. (1969).

The buoyant material (fig. 1) is a commercial detergent, Triton X–100, 10-percent concentration in water, whipped into a fine foam with a heavy duty Waring blender (e). The experiment consists of injecting an initial thermal into the tank and, after a specified delay time, injecting a second thermal into the wake of the first one. The camera operates continuously through the entire run. Figure 2 shows a typical sequence, with every other frame removed, for the nonrotation situation. It is obvious from the pictures in column II that the merging of the clouds prohibits quantitative photogrammetric reduction of the data beyond about the eighth second. The situation is worse for the rotation case; the vertical stretching of the clouds causes them to merge instantly and cover the full depth of the tank. As a consequence, quantitative measurements have not yet been made for the rotation case of successive thermals. Until this experimental difficulty can be overcome, the comparison with theory must be limited to consecutive thermals in a stationary medium and solitary thermals in a rotating medium.

Despite the difficulty with resolving photographically the boundaries between successive thermals, visual observations provide considerably more information about the nature of the interactions. For example, in the experiment depicted in figure 2, the initial thermal reaches the top of the tank in about 12 s. The first thermal was almost half way to the top when the second one was released (only the lower two-thirds of the tank shows in the photograph). Nevertheless, owing to the wake effect, the second thermal was able to rise through the initial one and reach the top of the tank ahead of it. Figure 3

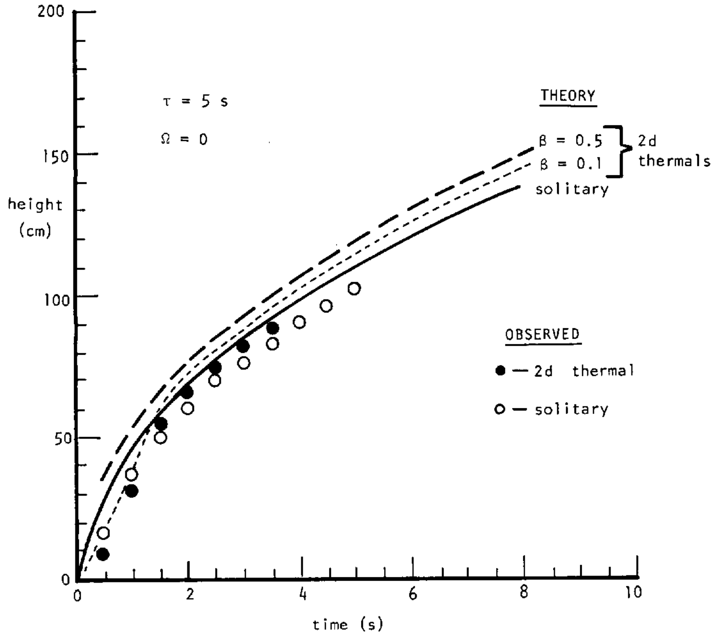

Figure 4.—Height of thermal cap versus time, nonrotation with 5-s time delay.

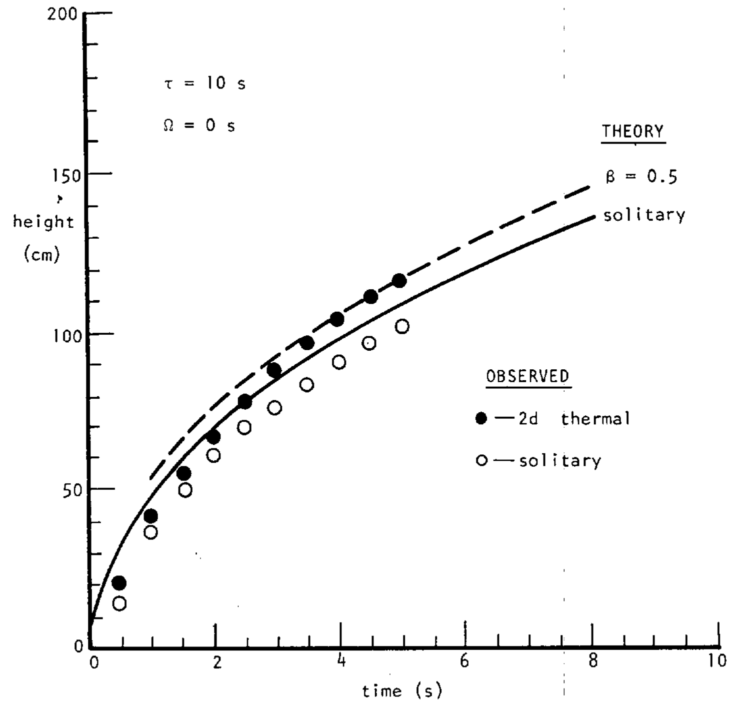

Figure 5.—Height of thermal cap versus time, nonrotation with 10-s time delay.

illustrates schematically the circulation patterns at the time that the second thermal penetrates the first. At this instant, the second thermal's peripheral downward flow counters the upward flow in the first one. As the second thermal emerges at the top, its entraining flow counters the divergent flow of the first one. By this time, the toroidal circulations of both thermals appear to have decayed extensively; but this might be due to the finite depth of the tank. Experiments in a deeper fluid are indicated as a possible way to resolve this uncertainty.

Visual observations also have provided some further information about consecutive thermals in a rotating medium. Qualitatively, at least, some aspects of the theory for strong interaction were verified. This case was simulated by bubbling air into the tank (fluid rotating as a solid) until a concentrated vortex formed; the velocity profile was then the irrotational type, although efforts to estimate the profile of tangential velocity from the depression of the fluid surface at the center of the tank were not successful. If the air bubbling is now stopped, the visibility in the tank will be satisfactory for injecting a "second" thermal. The vorticity field present at the time of injection may not be quite the same as one created by a single preceding thermal, but it should in fact be very much like the one assumed in deriving the theory for strong interaction. The second thermal seems to be separated into two parts. The inner part travels upward near the center of the tank at greatly enhanced vertical velocity, while the outer part is greatly suppressed. The relative size of each portion for a given injection depends somewhat upon the magnitude of the tank rotation rate Ω initially. According to the theory, enhancement or suppression occurs accordingly as the entrainment radius parameter is greater or less than a critical value. This indicates that the parameter γ may be a function of Ω, although this relationship is not yet well enough understood to be incorporated into the theory.

The plots of experimental data on the consecutive thermals are fitted by theoretical curves in such a manner as to obtain as much information as possible about the undetermined parameters of the theory. The entrainment constant α has been taken to be 0.2 for all of the theoretical computations; it was never found to vary significantly from this value in any of the experiments. This has also been the experience of other investigators. In plotting, all thermals are referred to a zero time base to facilitate comparison of the curves. Each data point represents an average for at least eight experiments.

Successive thermals without rotation. The injections for these thermals were 130 cm^3 of foam with a density of 0.20 g cm^{-3}, so that $F=10^5$ cm^4 s^{-2}. Figures 4 and 5 give the height of the thermal cap as a function of time for delay times of 5 and 10 s, respectively. Two values of β were used in figure 4 to see which curve might best fit the experimental data. Note that $\beta=0.1$ appears to predict best the amount of updraft enhancement of the rate of rise and also predicts correctly a crossover of the two curves. However, the crossover could be experimental error; and figure 5 for $\tau=10$ s shows better agreement for $\beta=0.5$. In fact, $\beta=0.1$ gives no enhancement of the second thermal after a 10-s time delay. If anything, β should be expected to decrease with the time delay between thermals;

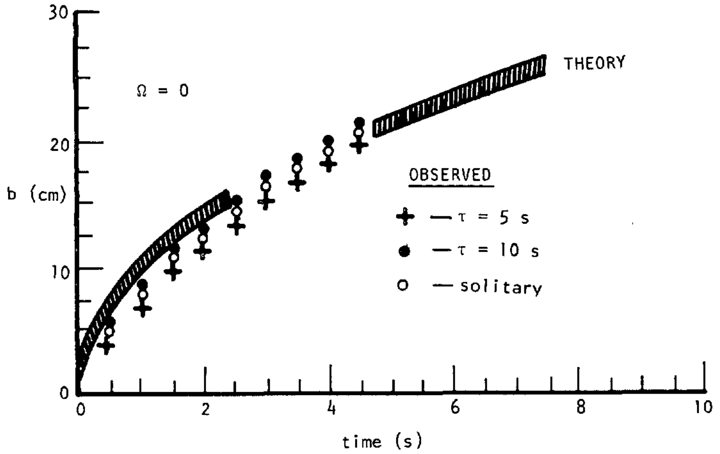

FIGURE 6.—Sphere-equivalent radius versus time, nonrotation with 5- and 10-s time delays.

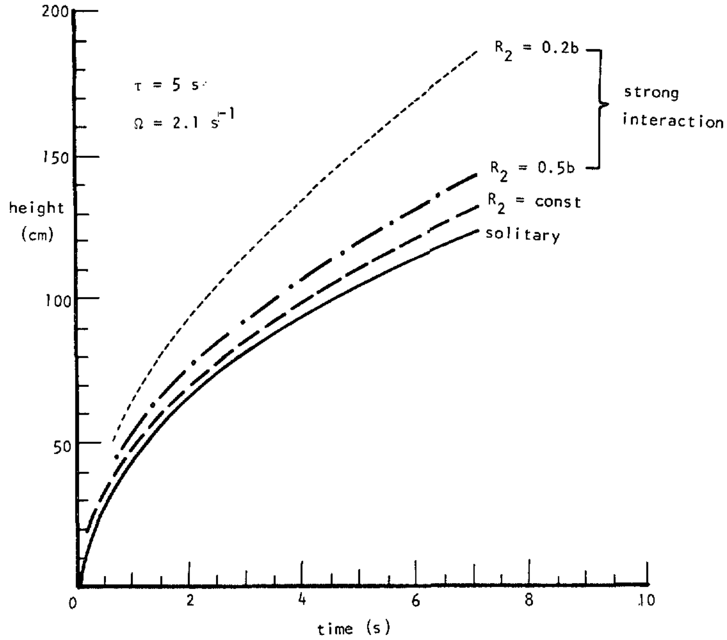

FIGURE 7.—Height of thermal cap versus time, rotation with 5-s time delay.

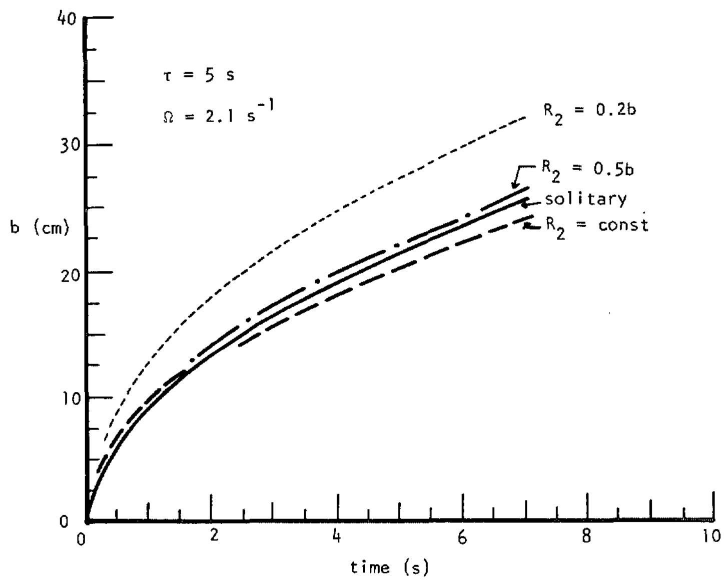

FIGURE 8.—Sphere-equivalent radius versus time, rotation with 5-s time delay.

and so, $\beta=0.5$ seems to be the best choice. This value is used for the remainder of the computations. The theoretical curves of b and h for this case were obtained from eq (24) and (31), respectively. No approximations were made in eq (24) for b, but the second thermal solutions for h in eq (31) are strictly valid only for $t<\tau$. Extension of the curves beyond $t=5$ min when $\tau=5$, however, does not appear to give any unreasonable trend to the curves.

The growth of the sphere-equivalent radius b is shown in figure 6. The variations predicted by theory for the three experimental situations plotted on figure 6 are included within the solid curve. The experimental data points also show a small range of variation, in agreement with theory.

Successive thermals with rotation. Theoretical calculations are made for this case for the purpose of comparing rotating with nonrotating thermals, even though experimental data are not available. The curves for the solitary thermal are calculated from eq (24) with $\beta=\tau=0$. The curves for second thermals with R_2=const are also calculated from eq (24) with $R_2=6$ cm. The curves for second thermals with strong interaction are calculated from eq (50) for two values of γ to show the range of rotation effects between $\gamma=0.2$ and $\gamma=0.5$. The entrainment radius for the first thermal is assumed to be $R_1=6$ cm in all cases, and the initial rotation rate is assumed to be $\Omega=2.1$ rad s^{-1}.

Figures 7 and 8 show the evolution of h and b, respectively, for $\tau=5$ s, and figures 9 and 10 are for $\tau=10$ s. In figure 7, the height h is seen to be increased relative to a solitary thermal for all rotation conditions, although the curve for R_2=const would show even more enhancement if rotation were not present. The curve for b in figure 8 shows a small amount of suppression of radial growth for R_2=const, as the rotation suppression effect dominates the residual updraft from the previous thermal.

The analysis for $\tau=10$ s correctly shows that the wake effect becomes less important for the longer time delay. Curves for h versus time and b versus time are all suppressed in figures 9 and 10 relative to their counterparts in figures 7 and 8, and both h and b are now suppressed relative to a solitary thermal. Figure 10 shows that, beyond the age of 5 s, the 10-s thermal for strong interaction and $\gamma=0.5$ has the same radius as a solitary thermal. As the time between thermals increases, the rotation suppression becomes more dominant over the updraft enhancement. We point out also that, for subcritical values of γ (greater than 0.526), the strong interaction theory will predict strong suppression rather than enhancement.

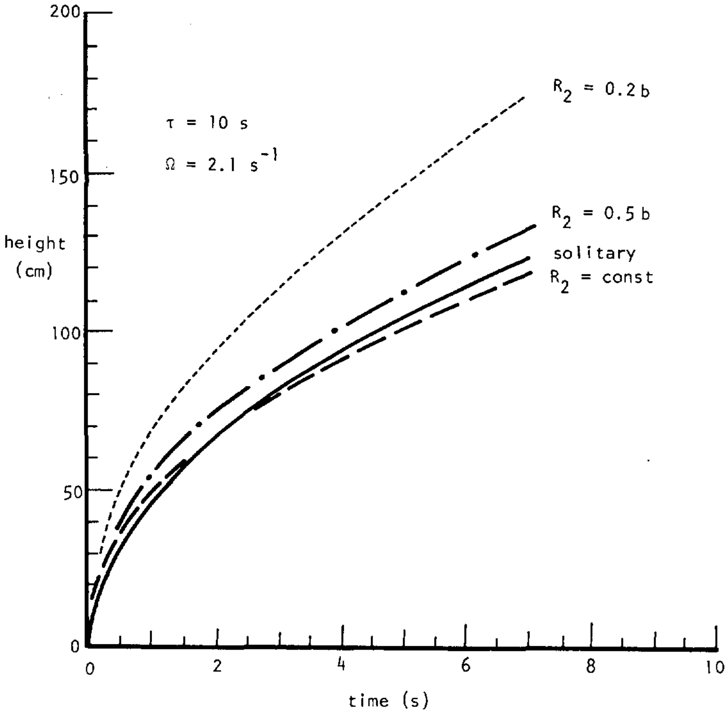

Figure 9.—Height of thermal cap versus time, rotation with 10-s time delay.

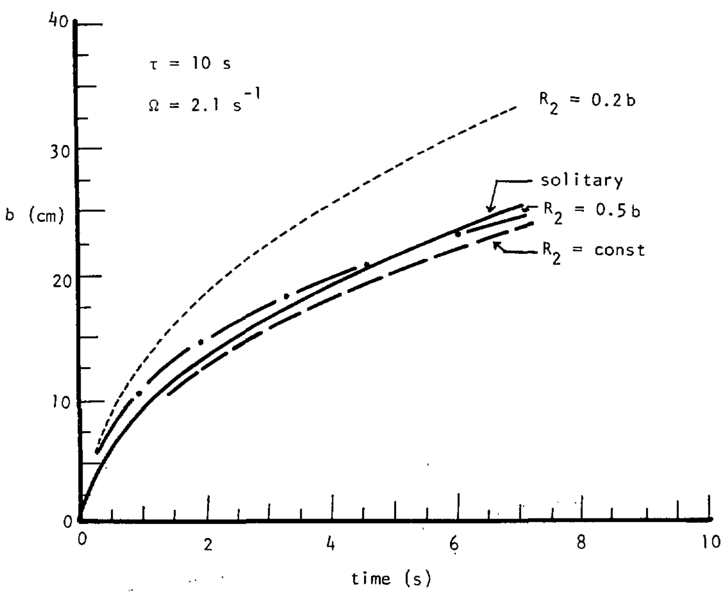

Figure 10.—Sphere-equivalent radius versus time, rotation with 10-s time delay.

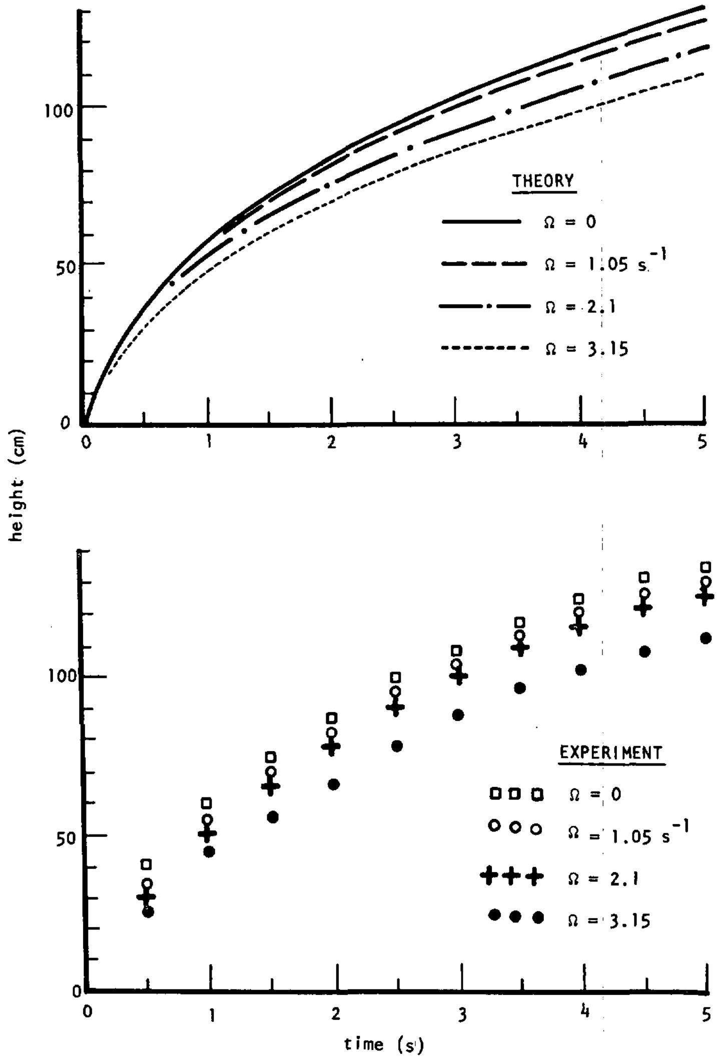

Figure 11.—Comparison of theory with the experiment for height of the thermal cap versus time, showing the suppression increasing with rotation rate.

It is important to note that the second thermal enhancements for strong interaction occur despite the fact that the first thermal is actually suppressed by the rotation field in each case. Figure 11 shows the amount of suppression of h for rotation rates of 1.05, 2.1, and 3.15 rad s^{-1} as predicted by eq (7) for solitary thermals. The entrainment radius R_1 is assumed to be 7.1 cm, to agree with data presented by Wilkins et al. (1969). The data points on the graph below these curves are for laboratory simulation experiments in which the injections are 300 cm^3 of foam with $F=2\times10^5$ cm^4 s^{-2}. The fit to the theoretical curves is excellent, and the curves agree well that the suppression increases with the magnitude of Ω.

We must also point out that the solution set (34) with $\gamma=0.5$, while oscillatory, will give close agreement with the experimental data points in figure 11 except for the highest rotation rate ($\Omega=3.15$ rad s^{-1}). The period of the oscillation is $\pi/\alpha\Lambda=15.8$ s for this case, and therefore set (34) predicts that the thermal will begin to descend after about 4 s. Since this is not observed experimentally, we are led to prefer the solution set (7) with R=const for the case of a solitary thermal in a rotating medium. Solution set (7) also predicts correctly that the entrainment rate will not be affected by rotation.

5. CONCLUSIONS

The treatment given here, albeit somewhat oversimplified, does have the advantage of demonstrating some of the most important processes associated with the interactions of successive thermals in a rotating medium. The theory takes into account the conservation of volume, momentum, and buoyancy in individual thermals and allows for a residual wake updraft between a thermal and its successor. The analysis is also suited to laboratory simulations where some of the parameters of such a complex phenomenon are subject to some degree of control; and in fact, the theory shows very good agreement with the experimental data where comparisons are possible.

The theory for strong interaction tells us that the vertical motion may be actually enhanced if the geometry of the situation is favorable, which is to say whenever the entrainment radius is small compared with the cloud radius. In this case, increasing the ambient rotation rate *further enhances* the vertical motion instead of suppressing it, as in the solutions obtained from eq (24).

Experiments in a deeper fluid are needed to observe at least two of the successive thermal processes that are prohibited with the present apparatus. One of these is the overtaking process, when one thermal passes through another, and the other is interactions between third and subsequent thermals. Certainly, if a second thermal differs substantially from the first thermal, then the wake of the second thermal must also be different from that of the first; and hence the third thermal must be different from the second, and so on. Some preliminary efforts have been made to extend the lifetime of thermals in the 183-cm tank by injecting thermals of smaller density deficit.

ACKNOWLEDGMENTS

The authors are indebted to Warren A. Meyer of the LTV Research Center, Dallas, Tex., for advice concerning the mathematical techniques used in this analysis. This research is supported by the Atmospheric Sciences Section, National Science Foundation, NSF Grant GA-16350.

REFERENCES

Chandrasekhar, Subrahmanyan, *Hydrodynamic and Hydromagnetic Stability*, Clarendon, Press, Oxford, England, **1961**, 652 pp. (see pp. 83–85).

Kuo, H. L., "On the Dynamics of Convective Atmospheric Vortices," *Journal of the Atmospheric Sciences*, Vol. 23, No. 1, Jan. **1966**, pp. 25–42.

Morton, B. R., Taylor, G. I., and Turner, J. S., "Turbulent Gravitational Convection From Maintained and Instantaneous Sources," *Proceedings of the Royal Society of London*, Ser. A, Vol. 234, No. 1196, England, Jan. **1956**, pp. 1–23.

Proudman, Joseph, "On the Motion of Solids in a Liquid Processing Vorticity," *Proceedings of the Royal Society of London*, Ser. A, Vol. 92, England, **1916**, pp. 408–424.

Scorer, Robert S., "Experiments on Convection of Isolated Masses of Buoyant Fluid," *Journal of Fluid Mechanics*, Vol. 2, Pt. 6, Taylor & Francis, Ltd., London, England, Aug. **1957**, pp. 583–594.

Taylor, Geoffrey Ingram, "Experiments With Rotating Fluids," *Proceedings of the Royal Society of London*, Ser. A, Vol. 100, England, **1921**, pp. 114–121.

Turner, J. S., "Model Experiments Relating to Thermals With Increasing Buoyancy," *Quarterly Journal of the Royal Meteorological Society*, Vol. 89, No. 379, London, England, Jan. **1963**, pp. 62–74.

Turner, J. S., "The Dynamics of Spheroidal Masses of Buoyant Fluid," *Journal of Fluid Mechanics*, Vol. 19, No. 4, Cambridge University Press, London, England, Aug. **1964**, pp. 481–490.

Wilkins, Eugene M., Sasaki, Yoshikazu, Friday, E. W., Jr., McCarthy, J., and McIntyre, J. R., "Properties of Simulated Thermals in a Rotating Fluid," *Journal of Geophysical Research, Oceans and Atmospheres*, Vol. 74, No. 18, Aug. 20, **1969**, pp. 4472–4486.

[*Received April 29, 1970; revised November 23, 1970*]